https://doi.org/10.5194/egusphere-2025-5184
Preprint. Discussion started: 1 December 2025

A potential explanation for the anomalously low nitrate to phosphate ratio in the well-oxygenated East/Japan Sea

Hyo-Ryeon Kim[1], Jae-Hyun Lim[2], Hae-Kun Jung[3], Jeong-Min Shim[4], Ju-Hyoung Kim[5], Seo-Young Kim[1], and Il-Nam Kim[1,*]

[1]Department of Marine Science, Incheon National University, Incheon, South Korea.
[2]Marine Environmental Research Division, National Institute of Fisheries Science, Busan, South Korea.
[3]Ocean climate and Ecology Research Division, National Institute of Fisheries Science, Busan 46083, South Korea.
[4]Fisheries Resources and Environment Division, East Sea Fisheries Research Institute, National Institute of Fisheries Science, Gangneung 25435, South Korea.
[5]Department of Aquaculture and Aquatic Science, Kunsan National University, Gunsan, South Korea.

Correspondence to: Il-Nam Kim (ilnamkim@inu.ac.kr)

Abstract. The East/Japan Sea (EJS), a well-oxygenated marginal sea, exhibits an anomalously low nitrate (NO_3^-) to phosphate (PO_4^{3-}) ratio (~12.6:1), diverging from the canonical Redfield ratio (16:1). To resolve this long-standing biogeochemical enigma, we examined nitrogen (N) cycling genes and bacterial communities across depths and seasons. External phosphorus inputs—riverine, atmospheric, and crustal—were insufficient to explain the imbalance. Instead, high abundances of N-reducing genes and affiliated taxa suggest a plausible role for bacterially mediated N loss throughout the water column. We propose that N removal may occur within particle-associated microenvironments (i.e., oxygen-depleted microzones inside sinking organic aggregates), despite oxygen-rich conditions. A dual-scale feedback—short-term anthropogenic N deposition enriching surface waters (i.e., increasing NO_3^-:PO_4^{3-} ratio in the upper waters) and longer-term deoxygenation, driven by the weakening of deep-water formation, potentially favoring subsurface N loss (i.e., decreasing NO_3^-:PO_4^{3-} ratio in the deep waters)—may promote a vertically stratified NO_3^-:PO_4^{3-} regime in the future EJS. Our findings highlight the EJS as a sentinel system for how combined anthropogenic and climatic forces could reshape marine nutrient balances.

Keywords
East/Japan Sea; Nitrogen cycling; nitrate to phosphate ratio; Redfield ratio; N-reducing genes; Nutrient imbalance; Dual-scale feedback; Anthropogenic and climatic forces

1 Introduction

The biogeochemical cycling of carbon (C), nitrogen (N), and phosphorus (P) in the ocean is tightly linked to phytoplankton growth, which depends on the availability of these essential elements (Arrigo, 2005). The elemental composition of marine organic matter, often described by the Redfield ratio (C:N:P=106:16:1), reflects a global coupling of biological nutrient uptake and remineralization (Redfield, 1958). The similarity between intracellular N:P ratios in phytoplankton and the surrounding seawater's nitrate (NO_3^-) to phosphate (PO_4^{3-}) ratio supports the idea that these elements are consumed and regenerated in near-constant proportions, stabilizing ocean nutrient stoichiometry.

The Redfield N:P ratio of 16:1 is often used to assess nutrient limitation and its effect on primary productivity. On geological timescales, biological dinitrogen (N_2) fixation (N_2 → particulate organic nitrogen; PON) and denitrification ($NO_3^- \rightarrow NO_2^- \rightarrow N_2O/N_2$) act as opposing forces that modulate the ocean's reactive N pool and maintain its global balance (Van Spanning et al., 2005), referred to as NO_3^-:PO_4^{3-} homeostasis (Gruber, 2008). These processes are key to regulating nutrient supply, biological productivity, and long-term carbon storage.

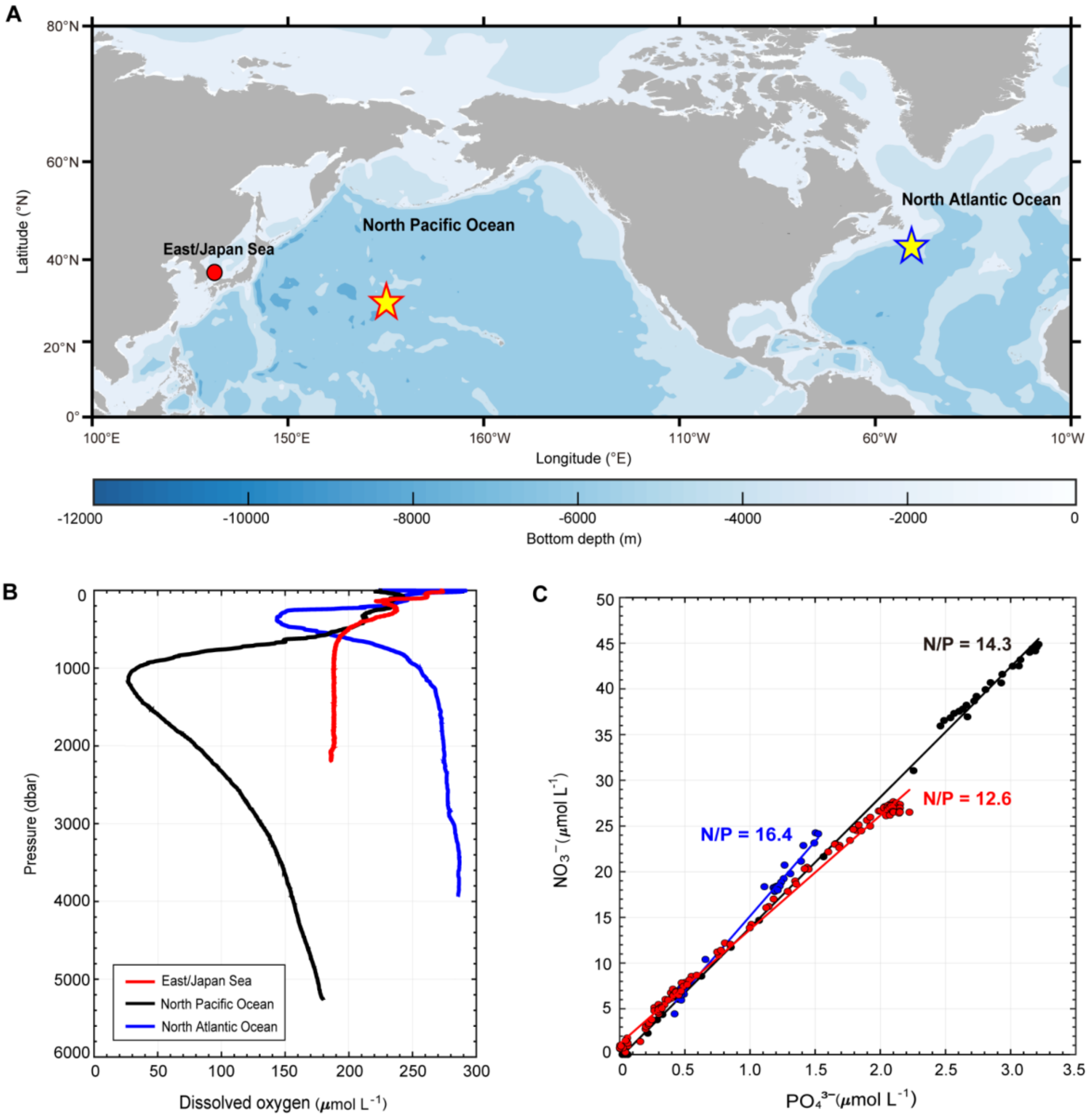

Figure 1: Dual oceanic traits of the East/Japan Sea. The East/Japan Sea (EJS) combines Atlantic-like oxygenation with Pacific-style nitrogen (N) scarcity, revealing a decoupling between redox structure and nutrient stoichiometry. (A) The sampling station in the Ulleung Basin, EJS (filled red circle), and reference stations in the North Pacific Ocean (NPO) and North Atlantic Ocean (NAO) (red- and blue-edged stars, respectively) are shown at comparable latitudes. (B) Vertical profiles of dissolved oxygen (μmol L^{-1}), and (C) NO_3^-: PO_4^{3-} ratios, are presented for each basin. Solid black, blue, and red lines represent the NPO, NAO, and EJS stations, respectively (This plot shows strong linear correlations in the NPO ($R^2 = 0.96$, $p < 0.05$), NAO ($R^2 = 0.95$, $p < 0.05$), and EJS ($R^2 = 0.92$, $p < 0.05$)). To contextualize the EJS biogeochemistry, DO, NO_3^- and PO_4^{3-} data from the ES were compared with reference profiles from station 76 (P02 section, North Pacific) and station 12 (A20 line, North Atlantic), retrieved from the CLIVAR and Carbon Hydrographic Data Office (CCHDO; https://cchdo.ucsd.edu).

Although the global NO_3^-:PO_4^{3-} ratio closely aligns with the Redfield ratio, significant regional deviations exist (Gruber, 2008) (Fig. 1A). For instance, in the North Atlantic Ocean (NAO), where deep convection and high oxygen concentrations prevail, the NO_3^-:PO_4^{3-} ratio exceeds 16:1, likely reflecting elevated N_2 fixation (Gruber and Sarmiento, 1997) (Fig. 1B and 1C). Conversely, in the North Pacific Ocean (NPO), where circulation terminates and oxygen concentrations are low, denitrification reduces the N inventory (Deutsch et al., 2001), leading to a lower NO_3^-:PO_4^{3-} ratio of ～14.3:1 (Fig. 1B and 1C). These variations highlight the regional imprint of biogeochemical processes on nutrient distributions.

The East/Japan Sea (EJS), a marginal sea in the northwest Pacific (Supplementary Fig. S1), is characterized by active deep-water formation and strong thermohaline circulation, frequently referred to as a 'Miniature Ocean' (Seung and Yoon, 1995). Despite its well-oxygenated conditions–comparable to those in the NAO–the EJS displays a remarkably low NO_3^-:PO_4^{3-} ratio of 12.6:1, lower even than that of the NPO (Fig. 1B and 1C). While some studies have proposed that denitrification might contribute to N loss in the EJS, definitive evidence is still lacking (Kim et al., 2012; Kim, 2015; Na et al. 2018). Consequently, the anomalously low NO_3^-:PO_4^{3-} ratio in the EJS has long remained a scientific enigma.

Much of our current understanding of marine N cycling derives from cultivation-based studies and stable isotope analyses. While these approaches have yielded important insights into microbial identities and transformation rates (Marchant et al., 2016), they are limited by the low cultivability of many marine microbes and the complex interpretation of isotopic data (Pace, 1997). Advances in molecular techniques, particularly 16S rRNA-based metagenomics, now enable the targeted use of bacterial biomarker genes to elucidate N cycling processes in marine environments (Lüke et al., 2016; Pajares and Ramos, 2019; Sharma et al., 2014).

Here, we present the first attempt to uncover potential clues to the anomalously low NO_3^-:PO_4^{3-}ratio in the well-oxygenated EJS, using bacterial biomarker genes and community compositions involved in N cycling. To this end, we conducted a research cruise in 2021, collecting water samples from five depths (0, 150, 300, 750, and 1000 m) over five months (February, April, June, August, and October). Our findings offer novel insights into microbial N cycling in well-oxygenated waters and contribute to resolving a long-standing biogeochemical enigma in the EJS.

2 Materials and Methods

2.1 Sampling and measurements of physical and biogeochemical parameters

Seawater samples for sequencing and physicochemical analysis were collected in the Ulleung Basin (UB) of the East Sea aboard R/V Tamgu 3 from February to October 2021 (Fig. 1A and Supplementary Fig. S1). Vertical profiles of temperature (T), salinity (S), and dissolved oxygen (DO) were measured from the surface (0m) to 1000 m using a Sea-Bird SBE 911plus CTD system equipped with a rosette sampler. Sensor accuracies were ± 0.001 °C for T, ± 0.0003 S m^{-1} for conductivity, and ± 2% for DO. Seawater samples for nutrients (NO_3^- and PO_4^{3-}) analyses were collected in acid-rinsed 15 mL vials and frozen at −20 °C. Nutrient concentrations were determined using a QuAAtro autoanalyzer (Seal Analytical, Germany) with analytical precision within 1%. For

DNA extraction, 2L of surface seawater was filtered through 0.22 µm cellulose ester membrane filters (Millipore, Ireland) to capture bacterial cells. Filtered samples were immediately frozen and subsequently stored at −80°C until DNA extraction.

2.2 Bacterial community composition and biomarker gene analysis

Genomic DNA was extracted from 2L of seawater filtered through 0.22 µm cellulose ester membranes (Millipore, Ireland). Total DNA was isolated using a DNA isolation kit (Qiagen, Germany) following the manufacturer's protocol, and the quality of the extracted DNA was verified with a NanoDrop spectrophotometer (Thermo Scientific, USA). After quality control, 16S rRNA sequencing libraries were constructed according to the Illumina 16S Metagenomic Sequencing Library Preparation protocol (Illumina, San Diego, CA, USA), targeting the V3–V4 hypervariable regions of the 16S rRNA gene. PCR amplification was performed with primers containing Illumina overhang adapters (Forward: 5′-TCGTCGGCAGCGTCAGATGTGTATAAGAGACAGCCTACGGGNGGCWGCAG-3′; Reverse: 5′-GTCTCGTGGGCTCGGAGATGTGTATAAGAGACAGGACTACHVGGGTATCTAATCC-3′;). The extracted DNA samples were sequenced on the Illumina MiSeq platform (2 × 300 bp paired-end, v3 chemistry) using MiSeq Control Software (v2.4.1.3) and Real-Time Analysis (RTA v1.18.54.0). Library preparation included limited-cycle PCR, indexing, normalization, and pooling, and 16S tagging of DNA fragments (100–300 bp) was performed using a quantitative DNA library preparation kit. Raw sequencing data were processed using QIIME 1.9.1, wherein paired-end reads were assembled into tags based on their overlapping regions. During the preprocessing stage, primers were trimmed, followed by demultiplexing and quality filtering (Phred ≥ 20). USEARCH7 was employed for denoising and chimera detection/filtering in operational taxonomic units (OTUs) clustering process. Then, OTUs were then assigned using the Silva132 and NCBI databases, with a 97% sequence similarity threshold via UCLUST and a close-reference clustering approach. OTU identifiers were established accordingly. The resulting OTU table was normalized by dividing each OTU count by the corresponding 16S rRNA gene copy number abundance. The filtered OTU table, in BIOM (Biological Observation Matrix) format, was subsequently clustered using the PyNAST (Python Nearest Alignment Space Termination) algorithm, applying a 97% similarity threshold. Taxonomic classification was conducted across multiple hierarchical levels, Phylum, Class, Order, Family, Genus, and Species, using the RDP classifiers. The relative abundance of phyla, classes, orders, families, genera, and species was estimated using the STAMP (Statistical Analysis of Metagenomic Profiles) program. Relative abundances of bacterial taxa were calculated as read counts normalized by predicted 16S rRNA gene copy number. In this study, bacterial community composition was analyzed at the order level. Functional profiling of bacterial sequences was performed using Tax4Fun2 (Wemheuer et al., 2020), a computational tool that infers functional attributes of bacterial communities from 16S rRNA gene data, leveraging the Ref99NR reference genome data base. Functional annotations were derived through comparison with Kyoto Encyclopedia of Genes and Genomes (KEGG) Orthology reference matrices from the KEGG database. The generated 16S rRNA sequence data have been deposited in the NCBI Sequence Read Archive (accession number: PRJNA1168283 and PRJNA1253365).

3 Results and Discussion

3.1 External phosphorus inputs are insufficient

The anomalously low NO_3^-:PO_4^{3-} ratio in the EJS may result from either an excess P supply or N loss. To assess the former, we evaluated all plausible external P sources, including riverine discharge, atmospheric deposition, and seawater-crust interaction. First, riverine discharge is a recognized vector for both particulate and dissolved P in marine environments (Withers and Jarvie, 2008). However, the EJS lacks major river systems capable of supplying significant P at the basin scale. In particular, discharge from Nakdong River–the most prominent riverine source in the region–is limited by the construction of a dam at its estuary (June 1990) and exhibits a low flow rate (mean: ~0.0004 Sv; 1 Sv = 10^6 m^3 sec^{-1}) (Yang et al., 2002). A seasonal alternative is the intrusion of Changjiang Discharge Water (CDW) from the East China Sea, which enters the southern EJS during summer (Supplementary Fig. S2) (Isobe et al., 2002). While the CDW may contain P, it is relatively enriched in N and confined to surface layers (Tseng et al., 2014). Furthermore, its influence has likely declined due to decreasing discharge volume (Myriokefalitakis et al., 2016). Together, these factors indicate that riverine P input to the EJS is spatially constrained, temporally limited, and minor in magnitude relative to N.

Second, atmospheric deposition can also contribute bioavailable P to surface waters via aerosols, mineral dust, and volcanic ash (i.e., particularly in regions influenced by volcanic activity) (Myriokefalitakis et al., 2016). The EJS lies downwind of heavily industrialized and densely populated areas of Northeast Asia, making it a potential recipient of anthropogenic emissions (Seo and Kim, 2023). However, recent studies have shown that since the 1980s, atmospheric deposition has led to a substantial increase in reactive N in the upper EJS (~0.24 μmol kg^{-1} yr^{-1}), resulting in a measurable rise in NO_3^- relative to PO_4^{3-} concentrations (Kim et al., 2014). This N-enriched atmospheric deposition can be excluded as a significant P source.

Lastly, seawater–crust interactions, particularly at hydrothermal vents under low-oxygen and high-temperature conditions, are known to release PO_4^{3-} into the water column (McManus et al., 1997). However, no hydrothermal activity has been identified within the EJS.

Taken together, these findings indicate that none of the plausible external P sources–riverine input, atmospheric deposition, or seawater–crust interaction–are sufficient to account for the anomalously low NO_3^-: PO_4^{3-} ratio observed in the EJS. Thus, increased P supply is unlikely to be the primary driver of the long-standing NO_3^-: PO_4^{3-} anomaly in the EJS.

3.2 Genetic and taxonomic evidence for N loss

Given that external P inputs are insufficient to explain the anomalously low NO_3^-: PO_4^{3-} ratio in the EJS, we next consider an alternative mechanism: N loss via bacterially mediated processes. In the marine N cycle, N loss is primarily driven by two bacterial pathways: NO_3^- reduction ($NO_3^- \xrightarrow[nap,\ nar]{} NO_2^-$), and denitrification ($NO_3^- \xrightarrow[nap,\ nar]{} NO_2^- \xrightarrow[nir]{} NO \xrightarrow[nor]{} N_2O \xrightarrow[nos]{} N_2$). These processes are catalyzed by key biomarker genes, including *nar*, *nap*, *nor*, *nir*, and *nos* (hereafter referred to as N-reducing genes; Fig. 2A).

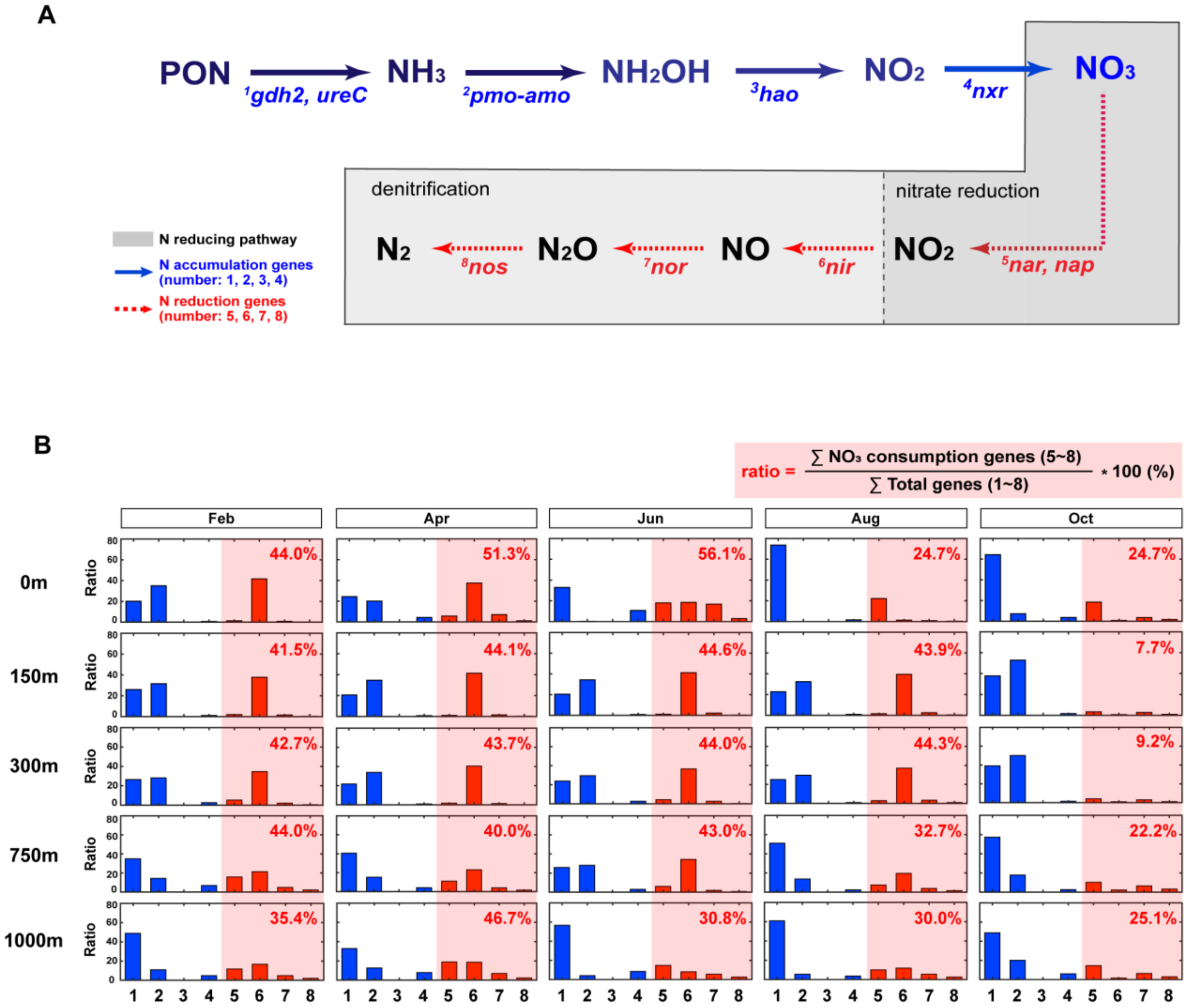

Figure 2: Temporal and depth-resolved structuring of nitrogen (N) reducing genes. (A) Blue solid arrows represent N-accumulation pathways, with associated genes (1–4) labeled beneath each arrow. In contrast, red dashed arrows indicate N reducing pathways, involving genes 5–8. Among these, nitrate reduction and denitrification—two major N-reducing pathways—are grouped within gray-shaded boxes. (B) The ratio of N-reducing gene abundance (genes 5–8) was calculated as the abundance of all transformation genes (genes 1–8), multiplied by 100. The resulting percentage is shown in red within each depth- and month-specific box.

To identity the extent of bacterially mediated N loss (i.e., N sinks), we analyzed the abundance of N-reducing genes and their associated bacterial communities across five depths (0, 150, 300, 750, and 1000 m) and five months (February, April, June, August, and October) in the EJS. The relative proportion (%) of N-reducing genes within the total N transformation gene pool (defined here as all analyzed N-cycling pathways including ammonification, nitrification, and denitrification genes) exhibited pronounced vertical and seasonal variability (Fig. 2B). From February to June, N-reducing genes accounted for 44.0–56.1% of the total N genes at the surface, decreasing steadily with depth to a minimum of 30.8% at 1000m. In August, surface abundance declined to 24.7%, while mid-depth layers (150–300m) showed elevated values of 43.9–44.3%, and deep layers (750–1000m) maintained moderate levels (30.0–32.7%). By October, abundances declined across all depths, reaching 7.7–9.2% at mid-depth. Temporal variability was particularly prominent at the surface and mid-depth layers, while the deep layers remained relatively stable (22.2–25.1%) (Supplementary Table S1).

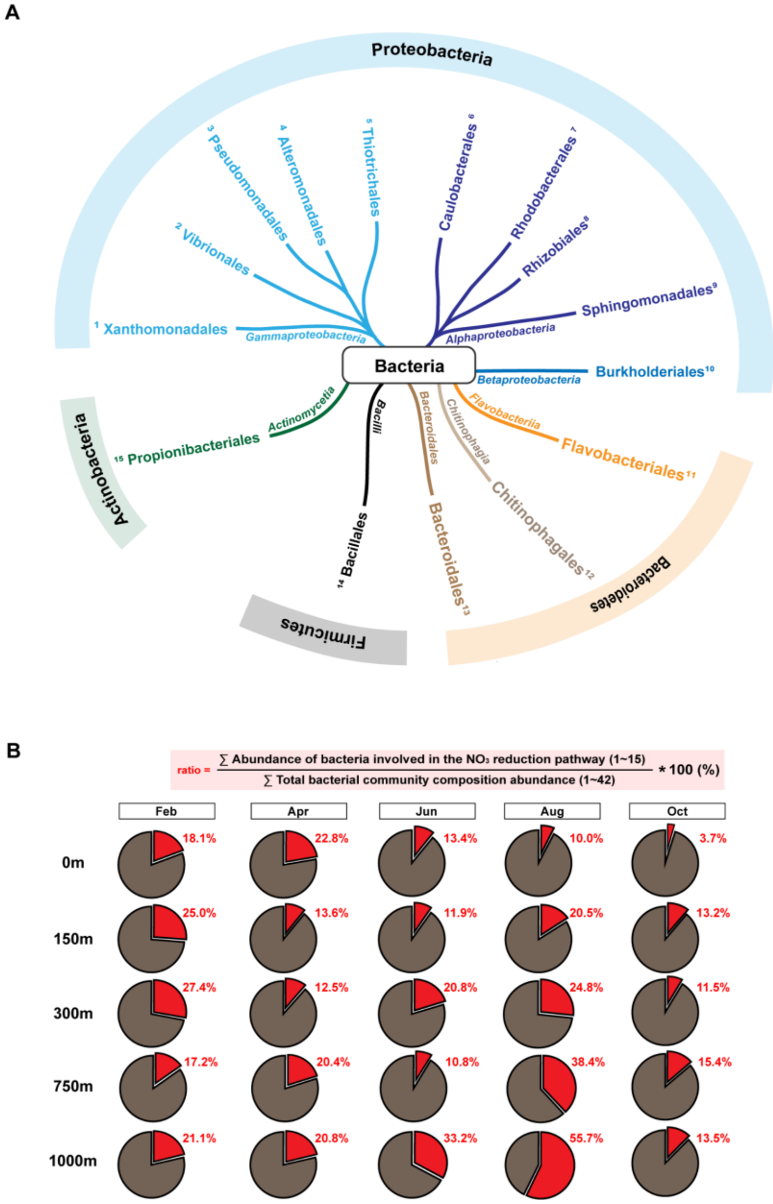

Figure 3: Spatiotemporal distribution of functionally grouped N-reducing bacterial communities. (A) Radial tree diagram for N-reducing 15 bacterial orders among 42 bacterial orders detected in the East/Japan Sea. Node colors represent class-level taxonomy, while node numbers (1–15) indicate bacterial orders functionally classified as N-reducing. (B) Proportion of N-reducing bacterial groups, calculated as the cumulative abundance of the 15 orders in (A), relative to the total abundance of all 42 bacterial orders identified in this study. The resulting ratio is shown as a red-colored segment in each pie chart, with numerical values annotated accordingly.

We further examined the relative abundance (%) of bacterial taxa at the order level that are potentially involved in N removal (hereafter referred to as N-reducing bacterial taxa) (Fig. 3). Of the 42 bacterial orders identified in the EJS (Supplementary Table S2), 15 were associated with N reduction pathways: three primarily associated with NO_3^- reduction (*Flavobacteriales*, *Caulobacteriales*, and *Thiotrichales*) (Starke et al., 2017), and twelve functionally linked to denitrification (*Rhodobacteriales*, *Alteromonadales*, *Pseudomonadales*, *Burkholderiales*, *Propionibacteriales*, *Bacillales*, *Rhizobiales*, *Chitinophagales*, *Bacteroidales*, *Vibrionales*, *Sphingobacteriales*, and *Xanthomonadales*) (Fujii et al., 2022; Podlesnaya et al., 2020; Russell et al., 2024; Starke et al., 2017; Wang et al., 2018; Wei et al., 2019; Wu et al., 2022) (Fig. 3A). In February, abundance increased with depth, from 18.1% at the surface to a maximum of 27.4% at 300 m, decreasing thereafter to 17.2–21.1% at 750–1000 m (Fig. 3B). In April, the opposite pattern emerged: surface abundance peaked at 22.8%, declining to 12.5% at 300 m, and stabilizing at 20.4–20.8% at deep layers. In June, abundance ranged from 10.8% to 20.8% between 0 and 750 m, followed by a sharp increase to 33.2% at 1000 m. In August, the lowest surface value (10.0%) coincided with a progressive increase with depth, culminating in the highest observed value (55.7%) at 1000 m. In contrast, October exhibited uniformly low abundances throughout the water column (3.7–15.4%), consistent with the distribution of N-reducing genes (Supplementary Table S3).

Overall, the mean proportions of N-reducing genes and their affiliated taxa across the study period were 37.7% and 20.0% (Supplementary Fig. S3), respectively, indicating the potential for bacterially mediated N loss in the EJS water column. As the actual rates of N loss via these pathways were not directly quantified, the study has limitations in quantitative interpretation. However, the combined gene and taxonomic evidence suggests that bacterially mediated N loss may contribute to the anomalously low NO_3^-: PO_4^{3-} ratio in the EJS.

3.3 How can N loss proceed in oxygenated waters?

Despite the well-oxygenated condition of the EJS water column ($O_2 > 180\ \mu mol\ L^{-1}$; Fig. 1B), our results suggest that N loss processes are likely to occur throughout the water column. This paradox may be reconciled by particle-associated microenvironments (i.e., oxygen-depleted microzones within sinking aggregates). The EJS combines high primary production with efficient vertical export, producing large, fast-sinking, highly porous aggregates and fecal pellets (Kwak et al., 2013; Otosaka et al., 2008). Within these particles, heterotrophic respiration consumes O_2 faster than it is replenished by diffusion, leading to steep O_2 gradients and suboxic–anoxic interiors at the millimeter scale, even while surrounding waters remain oxygenated (Alldredge and Cohen, 1987; Ploug et al., 1997). Previous studies have reported that benthic denitrification have also been detected along the Ulleung Basin margin (Kim et al., 2012; Na et al., 2018). However, the estimated benthic denitrification rates were insufficient to explain the persistently low basin-scale NO_3^-: PO_4^{3-} ratio in the EJS, indicating that additional N loss pathways in water column, such as particle-associated microenvironments, are likely involved. Global syntheses and modeling further show that such microenvironments extend the ecological niche for anaerobic metabolisms well beyond oxygen-minimum zones (OMZs) (Bianchi et al., 2018), resulting in the occurrence of N-loss pathways such as NO_3^- reduction and denitrification inside aggregate interiors (Alldredge and Silver, 1988). High abundances of N-reducing genes and taxa observed in the EJS are consistent with these mechanisms.

Similar cases of N loss in oxygenated waters have been reported across marine environments, particularly in (i) the eastern tropical North Pacific (ETNP), where laboratory experiments and a transect study showed denitrification within slowly sinking diatom aggregates in oxygenated seawater (Ciccarese et al., 2023); (ii) the northeast Pacific, where aggregate-linked NO_3^- respiration and denitrification were directly measured in oxygenated bottom waters ($O_2 > 100$ μmol L^{-1}), particularly during periods of high particle flux (Wolgast et al., 1998); (iii) the subtropical/temperate North Pacific, where N_2O isotopomer signatures detected in oxygenated waters are consistent with denitrification occurring within particle-associated microenvironments (Yamagishi et al., 2005); (iv) the South Pacific subtropical gyre, where basin-scale analyses along 32°S revealed measurable denitrification signals within the oxygen minimum layer (1100–2000 m), suggesting that particle-associated microzones may sustain N loss processes even in well-oxygenated open-ocean waters (Kim et al., 2013); and (v) oxygenated estuary–shelf waters of the Pearl River, Jiulong River, and Changjiang systems, where size-fractionated incubations implicate denitrification on larger particles as a dominant N_2O source (Wan et al., 2023). Our findings in the EJS align with these observations, indicating that oxygenated water columns do not necessarily preclude N removal—especially where and when particle-associated microenvironments exist.

3.4 Dual-scale feedbacks on the NO_3^-: PO_4^{3-} ratio

Our findings provide insight into the evolving biogeochemistry of the EJS under anthropogenic and climatic pressures that operate on distinct timescales and depth domains (Fig. 4).

In the surface layer, external N supply has increasingly been shaped by atmospheric N deposition rather than in situ N_2 fixation. Basin-scale analyses show a detectable rise of upper-ocean NO_3^- across the NPO, with the fastest increase in excess N relative to P (i.e., referred to as N^*) occurring in the EJS (～0.24 μmol kg^{-1} yr^{-1}) and a systematic decrease eastward with distance from Asian source regions—patterns consistent with the magnitude and distribution of atmospheric N deposition (Kim et al., 2014; Lee et al., 2020). This has produced an N-replete surface environment (i.e., a shift from N-limitation to P-limitation; see Supplementary Fig. S4). The anthropogenic signal emerged without concurrent changes in dissolved O_2 or P and does not require an increase in N_2 fixation, indicating atmospheric N deposition as the primary driver of the stoichiometric shift. As deposition continues, the surface NO_3^-:PO_4^{3-} ratio is likely to increase on shorter timescales, establishing a positive feedback that reinforces surface NO_3^- accumulation.

In deep waters, climate-driven processes appear to be reshaping nutrient dynamics over longer timescales. Historically, the EJS was ventilated by winter deep convection that renewed oxygen-rich bottom waters; however, tracer and hydrographic records indicate a mode shift in ventilation, from deep to predominantly intermediate-depth convection (~700–2000 m) (Gamo, 1999; Gamo et al., 2001; Kang et al., 2003). Over the same period, deep-water DO decreased by up to ~20 μM, and the oxygen-minimum layer deepened from a few hundred meters in the late 1960s to >1500 m by the 1990s—consistent with surface warming, reduced winter cooling, and strengthened stratification that reroutes ventilation to shallower layers (Kang et al., 2004; Kim et al., 2001). Although an exceptionally cold winter in 2000–2001 briefly re-initiated bottom-water renewal, the event was small and transient (≈0.03% of historical annual formation) (Kim et al., 2002; Talley et al., 2003). Forward modeling with a moving-boundary box framework further suggests that present bottom waters will be replaced by deep/central waters by ~2040, implying continued oxygen decline

(Kang et al., 2003; Kang et al., 2004). Together, these changes plausibly favor particle-associated microenvironments that mediate N loss, gradually depleting the deep NO_3^- inventory and lowering the deep $NO_3^-:PO_4^{3-}$ ratio (e.g., $NO_3^-:PO_4^{3-}{}_{1999} = 13.0 > NO_3^-:PO_4^{3-}{}_{2021} = 12.6$; see Supplementary Fig. S4).

Together, these dual-scale feedbacks—surface N enrichment driven by anthropogenic N deposition (short-term: increasing $NO_3^-:PO_4^{3-}$ ratio in the upper waters) and subsurface N removal associated with climate-driven deoxygenation (long-term: decreasing $NO_3^-:PO_4^{3-}$ ratio in the deep waters)—may create a vertically stratified $NO_3^-:PO_4^{3-}$ regime in the future EJS. Given this dual sensitivity, the EJS may serve as a sentinel for biogeochemical responses in other marine environments.

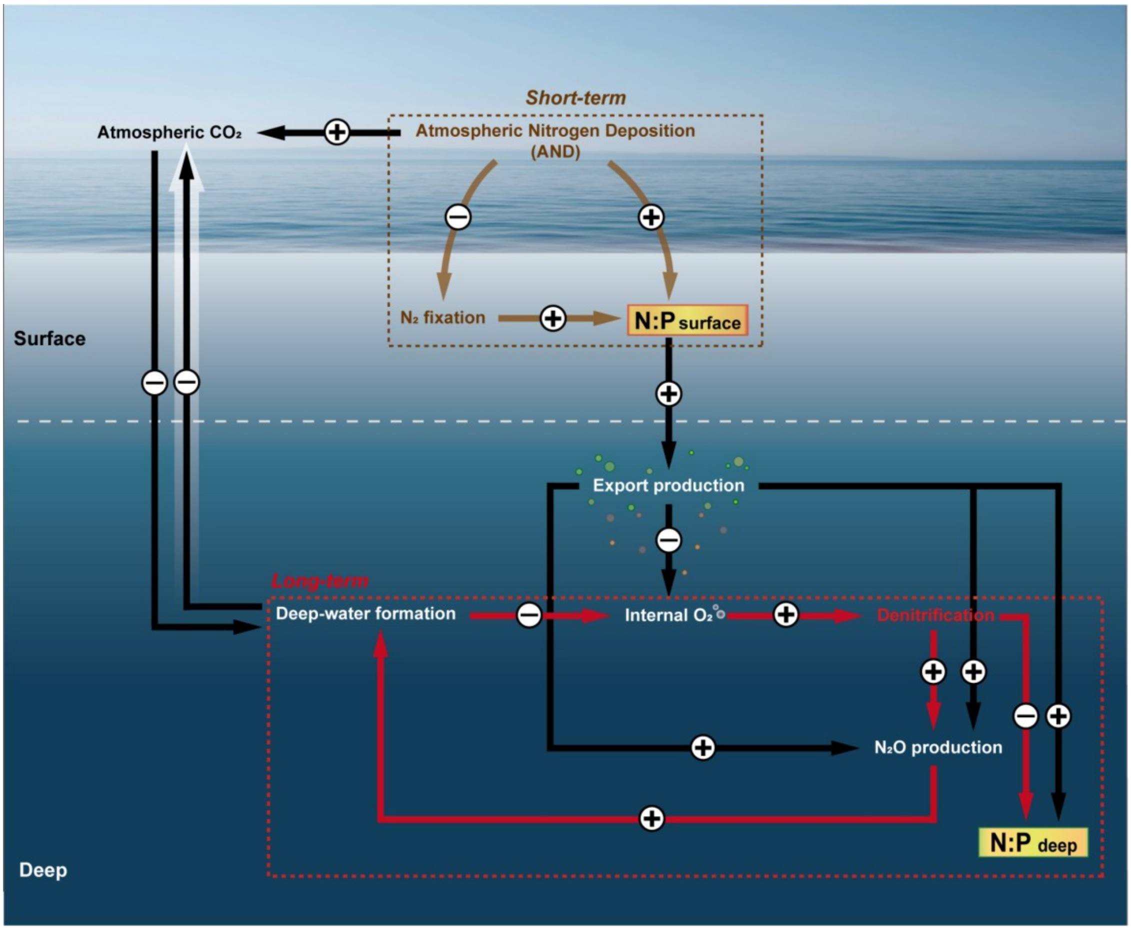

Figure 4: Conceptual schematic summarizing external drivers influencing the $NO_3^-:PO_4^{3-}$ ratio in the East/Japan Sea. The schematic illustrates a simplified pathway showing the sequential influences on the $NO_3^-:PO_4^{3-}$ ratio, driven by two key external factors: atmospheric N deposition, acting as a short-term driver (brown dashed box), and climate-induced suppression of deep-water formation, representing a long-term driver (red dashed box). Arrows indicate potential intermediate links among processes. A plus sign (+) denotes enhancement, whereas a minus sign (–) indicates suppression of the process.

https://doi.org/10.5194/egusphere-2025-5184
Preprint. Discussion started: 1 December 2025

3.5 Caveats and Future directions

While our study provides a plausible explanation for the anomalously low NO_3^-:PO_4^{3-} ratio in the East/Japan Sea (EJS), several caveats must be emphasized. First, our inference of bacterially mediated N loss is derived from genetic and taxonomic evidence rather than direct rate measurements. Although the high relative abundances of N-reducing genes and affiliated taxa suggest the potential for active denitrification, the actual magnitude of N loss remains unconstrained. Future studies should therefore incorporate direct process-rate determinations, such as N isotope tracer incubations, in situ microsensor profiling within sinking aggregates, and sediment-trap experiments to quantify particle-associated N loss more precisely. Second, the spatiotemporal variability of oxygen-depleted microenvironments in the EJS remains poorly characterized. The formation, persistence, and turnover of such microzones likely vary with aggregate composition, particle flux intensity, and seasonal productivity, yet these dynamics were not resolved here. High-resolution time-series observations that integrate biological, chemical, and physical measurements will be essential to capture these short-lived but biogeochemically significant microenvironments. Finally, the EJS should be considered not only a regional anomaly but also a testbed for broader climate–biogeochemistry feedbacks. Comparative studies across other well-oxygenated marginal seas and open-ocean settings are urgently needed to evaluate whether particle-associated microenvironments constitute a widespread and underappreciated sink for fixed N. Such efforts, combining multi-omics approaches with direct rate measurements and coupled physical–biogeochemical models, will be critical for predicting how anthropogenic nutrient inputs and climate-driven deoxygenation jointly reshape the global N cycle.

4 Summary and Conclusions

The EJS, which is a well-oxygenated marginal sea, exhibits an anomalously low NO_3^-:PO_4^{3-} ratio (12.6:1), deviating from the canonical Redfield ratio (16:1). External P inputs are insufficient to explain this anomaly. Instead, N-reducing genes and taxa suggest that bacterially mediated N loss is a plausible contributing factor, potentially occurring in particle-associated microenvironments (i.e., oxygen-depleted microzones in sinking aggregates). We propose a dual-scale feedback: short-term anthropogenic N deposition enriches surface waters (i.e., increasing NO_3^-:PO_4^{3-} ratio in the upper waters), while longer-term climate-driven deoxygenation could promote subsurface N loss (i.e., decreasing NO_3^-:PO_4^{3-} ratio in the deep waters). This combination may result in a vertically stratified stoichiometric regime in the future EJS. The EJS thus serves as a sentinel system, illustrating how concurrent human and climatic pressures may reshape marine nutrient cycling and offering insight into future changes in global ocean biogeochemistry.

Authorship contribution statement

Hyo-Ryeon Kim: Conceptualization, Software, Writing - Original Draft, Visualization. **Jae-Hyun Lim:** Conceptualization, Validation, Investigation. **Hae-Kun Jun:** Conceptualization, Validation, Investigation, Data curation. **Jeong-Min Shim:** Conceptualization, Validation, Investigation. **Ju-Hyoung Kim:** Conceptualization, Validation, Writing - Review & Editing. **Seo-Young Kim:** Software, Validation. **Il-Nam Kim:** Conceptualization, Writing - Original Draft, Validation, Supervision.

Funding

This study was supported by National Research Foundation of Korea (NRF) funded by Korean government (MSIT) (NRF-2022R1A2C1008475) and National Institute of Fisheries Science (NIFS), MOF, Korea (R2025015).

Declaration of competing interest

The authors declare that they have no known competing financial interests or personal relationships that could have appeared to influence the work reported in this paper.

Acknowledgements

We would like to thank the captain and crew members of the R/V Tamgu 3 for their endless support during the 2021 cruises.

Data availability

Data will be made available on request.

Appendix A. Supplementary materials

The supplementary materials (Figs. S1–4 and Table S1–3) are found in the submitted files.

References

Alldredge, A. L., and Cohen, Y.: Can microscale chemical patches persist in the sea? Microelectrode study of marine snow, fecal pellets, *Science*, **235**(4789), 689–691, https://doi.org/10.1126/science.235.4789.689, 1987.

Alldredge, A. L., and Silver, M. W.: Characteristics, dynamics and significance of marine snow, *Prog. Oceanogr.*, **20**(1), 41–82, https://doi.org/10.1016/0079-6611(88)90053-5, 1988.

Arrigo, K. R.: Marine microorganisms and global nutrient cycles, *Nature*, **437**(7057), 349–355. https://doi.org/10.1038/nature04159, 2005.

Bianchi, D., Weber, T. S., Kiko, R., and Deutsch, C.: Global niche of marine anaerobic metabolisms expanded by particle microenvironments, *Nat. Geosci.*, **11**(4), 263–268, https://doi.org/10.1038/s41561-018-0081-0, 2018.

Ciccarese, D., Tantawi, O., Zhang, I. H., Plata, D., and Babbin, A. R.: Microscale dynamics promote segregated denitrification in diatom aggregates sinking slowly in bulk oxygenated seawater, *Commun. Earth Environ.*, **4**(1), 275, https://doi.org/10.1038/s43247-023-00935-x, 2023.

Deutsch, C., Gruber, N., Key, R. M., Sarmiento, J. L., and Ganachaud, A.: Denitrification and N_2 fixation in the Pacific Ocean, *GLOBAL BIOGEOCHEM CY.*, **15**(2), 483–506, https://doi.org/10.1029/2000GB001291, 2001.

Fujii, N., Kuroda, K., Narihiro, T., Aoi, Y., Ozaki, N., Ohashi, A., and Kindaichi, T.: Metabolic potential of the superphylum Patescibacteria reconstructed from activated sludge samples from a municipal wastewater treatment plant, *M&E.*, **37**(3), ME22012, https://doi.org/10.1264/jsme2.ME22012, 2022.

Gamo, T.: Global warming may have slowed down the deep conveyor belt of a marginal sea of the northwestern Pacific: Japan Sea, *Geophys. Res. Lett.*, **26**(20), 3137–3140, https://doi.org/10.1029/1999GL002341, 1999.

Gamo, T., Momoshima, N., and Tolmachyov, S.: Recent upward shift of the deep convection system in the Japan Sea, as inferred from the geochemical tracers tritium, oxygen, and nutrients, *Geophys. Res. Lett.*, **28**(21), 4143–4146, https://doi.org/10.1029/2001GL013367, 2001.

Gruber, N.: The marine nitrogen cycle: overview and challenges, in: Nitrogen Marine Environment, edited by: Douglas, G. C., Deborah, A. B., Margaret, R. M., and Edward, J. C., Elsevier Science & Technology, Oxford, UK, 1–50, ISBN: 978–0–12–372522–6, 2008.

Gruber, N., and Sarmiento, J. L.: Global patterns of marine nitrogen fixation and denitrification, *GLOBAL BIOGEOCHEM CY.*, **11**(2), 235–266, https://doi.org/10.1029/97GB00077, 1997.

Isobe, A., Ando, M., Watanabe, T., Senjyu, T., Sugihara, S., and Manda, A.: Freshwater and temperature transports through the Tsushima-Korea Straits, *J. Geophys. Res. Oceans.*, **107**(C7), 2–1, https://doi.org/10.1029/2000JC000702, 2002.

Kang, D. J., Park, S., Kim, Y. G., Kim, K., and Kim, K. R.: A moving-boundary box model (MBBM) for oceans in change: An application to the East/Japan Sea, *Geophys. Res. Lett.*, **30**(6), https://doi.org/10.1029/2002GL016486, 2003.

Kang, D. J., Kim, J. Y., Lee, T., and Kim, K. R.: Will the East/Japan Sea become an anoxic sea in the next century?, *Mar. Chem.*, **91**(1–4), 77–84, https://doi.org/10.1016/j.marchem.2004.03.020, 2004.

Kim, I. N., Min, D. H., and Lee, T.: Deep Nitrate Deficit Observed in the Highly Oxygenated East/Japan Sea and Its Possible Cause, *Terr. Atmos. Ocean. Sci.* **23**, 671–683, https://doi.org/10.3319/TAO.2012.08.11.01(Oc), 2012.

Kim, I. N., Min, D. H., and Macdonald, A. M.: Water column denitrification rates in the oxygen minimum layer of the Pacific Ocean along 32S, *Global Biogeochem Cy.*, **27**(3), 816–827, https://doi.org/10.1002/gbc.20070, 2013.

Kim, I. N., Lee, K., Gruber, N., Karl, D. M., Bullister, J. L., Yang, S., and Kim, T. W.: Increasing anthropogenic nitrogen in the North Pacific Ocean, *Science*, **346**(6213), 1102–1106, https://doi.org/10.1126/science.1258396, 2014.

Kim, I. N.: Estimating Denitrification Rates in the East/Japan Sea Using Extended Optimum Multi-Parameter Analysis, *Terr. Atmos. Ocean. Sci*, **26**, https://doi.org/10.3319/TA0.2014.09.24.01(Oc), 2015.

Kim, K., Kim, K. R., Min, D. H., Volkov, Y., Yoon, J. H., and Takematsu, M.: Warming and structural changes in the East (Japan) Sea: a clue to future changes in global oceans?, *Geophys. Res. Lett.*, **28**(17), 3293–3296, https://doi.org/10.1029/2001GL013078, 2001.

Kim, K. R., Kim, G., Kim, K., Lobanov, V., Ponomarev, V., and Salyuk, A.: A sudden bottom-water formation during the severe winter 2000–2001: The case of the East/Japan Sea, *Geophys. Res. Lett.*, **29**(8), 75–1, https://doi.org/10.1029/2001GL01449, 2002.

Kwak, J. H., Lee, S. H., Park, H. J., Choy, E. J., Jeong, H. D., Kim, K. R., and Kang, C. K.: Monthly measured primary and new productivities in the Ulleung Basin as a biological" hot spot" in the East/Japan Sea, *Biogeosciences*, **10**(7), 4405–4417, https://doi.org/10.5194/bg-10-4405-2013, 2013.

Lee, K., Lee, E., and Lee, C. H.: Anthropogenic Perturbations of the Carbon and Nitrogen Cycles in the East Sea (Sea of Japan), in: Changing Asia-Pacific Marginal Seas, edited by: Chen, C. T., and Guo, X., 87–103 pp., Springer, Singapore, https://doi.org/10.1007/978-981-15-4886-4_6, 2020.

Lüke, C., Speth, D. R., Kox, M. A., Villanueva, L., and Jetten, M. S.: Metagenomic analysis of nitrogen and methane cycling in the Arabian Sea oxygen minimum zone, PeerJ, 4, e1924, https://doi.org/10.7717/peerj.1924, 2016.

Marchant, H. K., Mohr, W., and Kuypers, M. M.: Recent advances in marine N-cycle studies using 15N labeling methods, *Curr. Opin. Biotech.*, **41**, 53–59, https://doi.org/10.1016/j.copbio.2016.04.019, 2016.

McManus, J., Berelson, W. M., Coale, K. H., Johnson, K. S., and Kilgore, T. E.: Phosphorus regeneration in continental margin sediments, *Geochim. Cosmochim. Acta.*, **61**(14), 2891–2907, https://doi.org/10.1016/S0016-7037(97)00138-5, 1997.

Myriokefalitakis, S., Nenes, A., Baker, A. R., Mihalopoulos, N., and Kanakidou, M.: Bioavailable atmospheric phosphorous supply to the global ocean: a 3-D global modeling study, *Biogeosciences*, **13**, 6519–6543, https://doi.org/10.5194/bg-13-6519-2016, 2016.

Na, T., Thamdrup, B., Kim, B., Kim, S. H., Vandieken, V., Kang, D. J., and Hyun, J. H.: N_2 production through denitrification and anammox across the continental margin (shelf–slope–rise) of the Ulleung Basin, East Sea, *Limnol. Oceanogr.*, **63**(S1), S410–S424, https://doi.org/10.1002/lno.10750, 2018.

Otosaka, S., Tanaka, T., Togawa, O., Amano, H., Karasev, E. V., Minakawa, M., and Noriki, S.: Deep sea circulation of particulate organic carbon in the Japan Sea, *J. Oceanogr.*, **64**(6), 911–923, https://doi.org/10.1007/s10872-008-0075-4, 2008.

Pace, N. R.: A molecular view of microbial diversity and the biosphere, *Science*, **276**(5313), 734–740, https://doi.org/10.1126/science.276.5313.734, 1997.

Pajares, S., and Ramos, R.: Processes and microorganisms involved in the marine nitrogen cycle: knowledge and gaps, *Front. Mar. Sci.*, **6**, 739, https://doi.org/10.3389/fmars.2019.00739, 2019.

Ploug, H., Kühl, M., Buchholz-Cleven, B., and Jørgensen, B. B.: Anoxic aggregates-an ephemeral phenomenon in the pelagic environment?, *Aquat. Microb. Ecol.*, **13**(3), 285–294, https://doi.org/10.3354/ame013285, 1997.

Podlesnaya, G. V., Potapov, S. A., Krasnopeev, A. Y., Shtykova, Y. R., Tomberg, I. V., Timoshkin, O. A., and Belykh, O. I.: Diversity of denitrifying bacteria in biofilms formed on stony substrates of the lake Baikal Littoral Zone, *Microbiol.*, **89**(3), 369–373, https://doi.org/10.1134/S0026261720030133, 2020.

Redfield, A. C.: The biological control of chemical factors in the environment, *Am. Sci.*, **46**(3), 230A–221, http://www.jstor.org/stable/27827150, 1958.

Russell, M. V., Messer, T. L., Repert, D. A., Smith, R. L., Bartelt-Hunt, S., Snow, D. D., and Reed, A. P.: Influence of Four Veterinary Antibiotics on Constructed Treatment Wetland Nitrogen Transformation, *Toxics*, **12**(5), 346, https://doi.org/10.3390/toxics12050346, 2024.

Seo, H., and Kim, G.: Anthropogenic iron invasion into the ocean: Results from the East Sea (Japan Sea), *ES&T*, **57**(29), 10745–10753, https://doi.org/10.1021/acs.est.3c01084, 2023.

Seung, Y. H., and Yoon, J. H.: Some features of winter convection in the Japan Sea, *J. Oceanogr.,* **51**(1), 61–73, https://doi.org/10.1007/BF02235936, 1995.

Sharma, V., Chetal, G., Taylor, T. D., and Prakash, T.: Metagenomics of the Microbial Nitrogen Cycle: Functional Assignment of Metagenomic Data: Insights for the Microbial Nitrogen Cycle, Edited by: Diana Marco, Caister Academic Press, UK, 1–15, ISBN 978-1-908230-60-7, 2014.

Starke, R., Müller, M., Gaspar, M., Marz, M., Küsel, K., Totsche, K. U., Bergen, M., and Jehmlich, N.: Candidate Brocadiales dominates C, N and S cycling in anoxic groundwater of a pristine limestone-fracture aquifer, *J Proteomics*, **152**, 153–160, https://doi.org/10.1016/j.jprot.2016.11.003, 2017.

Talley, L. D., Lobanov, V., Ponomarev, V., Salyuk, A., Tishchenko, P., Zhabin, I., and Riser, S.: Deep convection and brine rejection in the Japan Sea, *Geophys. Res. Lett.*, **30**(4), https://doi.org/10.1029/2002GL016451, 2003.

Tseng, Y.-F., Lin, J., Dai, M., and Kao, S.-J.: Joint effect of freshwater plume and coastal upwelling on phytoplankton growth off the Changjiang River, *Biogeosciences*, **11**, 409–423, https://doi.org/10.5194/bg-11-409-2014, 2014.

Van Spanning, R. J. M., Delgado, M. J., and Richardson, D. J.: The nitrogen cycle: denitrification and its relationship to N_2 fixation, in: Nitrogen fixation in agriculture, forestry, ecology, and the environment, edited by: Werner, D., and Newton, W. E., Springer, Dordrecht, Netherlands, 277–342, https://doi.org/10.1007/1-4020-3544-6_13, 2005.

Wan, X. S., Sheng, H. X., Liu, L., Shen, H., Tang, W., Zou, W., Xu, M. N., Zheng, Z., Tan, E., Chen, M., Zhang, Y., Ward, B. B., and Kao, S. J.: Particle-associated denitrification is the primary source of N_2O in oxic coastal waters, *Nat. Commun.*, **14**(1), 8280, https://doi.org/10.1038/s41467-023-43997-3, 2023.

Wang, X., Ye, C., Zhang, Z., Guo, Y., Yang, R., and Chen, S.: Effects of temperature shock on N_2O emissions from denitrifying activated sludge and associated active bacteria, *Bioresource technology,* **249***,* 605–611, https://doi.org/10.1016/j.biortech.2017.10.070, 2018.

Wei, Z. S., Wang, J. B., Huang, Z. S., Xiao, X. L., Tang, M. R., Li, B. L., and Zhang, X.: Removal of nitric oxide from biomass combustion by thermophilic nitrification-aerobic denitrification combined with catalysis in membrane biofilm reactor, *Biomass Bioenergy*, **126**, 34–40, https://doi.org/10.1016/j.biombioe.2019.05.004, 2019.

Wemheuer, F., Taylor, J. A., Daniel, R., Johnston, E., Meinicke, P., Thomas, T., and Wemheuer, B.: Tax4Fun2: prediction of habitat-specific functional profiles and functional redundancy based on 16S rRNA gene sequences, *Environ. microbiome.*, **15**(1), 11, https://doi.org/10.1186/s40793-020-00358-7, 2020.

Withers, P. J. A., and Jarvie, H. P.: Delivery and cycling of phosphorus in rivers: a review, *Sci. Total Environ.*, **400**(1–3), 379–395, https://doi.org/10.1016/j.scitotenv.2008.08.002, 2008.

Wolgast, D. M., Carlucci, A. F., and Bauer, J. E.: Nitrate respiration associated with detrital aggregates in aerobic bottom waters of the abyssal NE Pacific, *Deep-Sea Res. II: Top. Stud. Oceanogr.*, **45**(4–5), 881–892, https://doi.org/10.1016/S0967-0645(98)00006-X, 1998.

Wu, M., Zhang, Z., Zhang, X., Dong, L., Liu, C., and Chen, Y.: Propionibacterium freudenreichii-Assisted approach reduces N_2O emission and improves denitrification via promoting substrate uptake and metabolism, *ES&T.*, **56**(23), 16895–16906, https://doi.org/10.1021/acs.est.2c05674, 2022.

Yang, H. S., Hwang, D. W., and Kim, G.: Factors controlling excess radium in the Nakdong River estuary, Korea: submarine groundwater discharge versus desorption from riverine particles, *Mar. Chem.*, **78**(1), 1–8, https://doi.org/10.1016/S0304-4203(02)00004-X, 2002.

Yamagishi, H., Yoshida, N., Toyoda, S., Popp, B. N., Westley, M. B., and Watanabe, S.: Contributions of denitrification and mixing on the distribution of nitrous oxide in the North Pacific, *Geophys. Res. Lett.*, **32**(4), https://doi.org/10.1029/2004GL021458, 2005.